1998

Coupled Hydrocode Prediction of Underwater Explosion Damage

Andrew Wardlaw, Jr., Reid McKeown and Alan Luton
Naval Surface Warfare Center, Indian Head Division
Warhead Performance and Lethality Division, Code 420
101 Strauss Avenue, Indian Head MD 20640-5035
andrewwardlaw@uwtech.ih.navy.mil

Damage to a deformable underwater target is difficult to predict as a consequence of the stiffness of water. Targets that deform inwards create an additional volume that must be filled by the surrounding water, reducing the local pressure and unloading the structure. To capture this behavior for close-in explosions requires a coupled fluid and structure analysis. The following paper describes such a coupled analysis and compares results to experiments on water filled cylinders. Examination of computation and experiment indicates that cavitation and the cavitation collapse play an important role in the cylinder transient flow field. Predicted mid-line pressure, velocity and deformation are in reasonable agreement with experiment. Numerical experiments indicate that uncertainties in the water equation of state, material model and explosive energy can have a significant influence on predicted velocities and deformations.

1. Introduction

Accurate prediction of underwater explosion damage against surface ships and submarines is an important aspect of naval weapon system design. The stiffness of water makes this a difficult problem; deformation of the target modifies the pressure in the surrounding fluid, changing the explosive loading. As a consequence, it is necessary to couple the fluid/explosive modeling with the structure simulation. Thus, the underwater damage prediction problem is complex, extremely non-linear and target deformation can alter effective load imposed by a weapon.

Methods of attacking underwater explosion damage prediction range from experiment to hydrocode simulation. Unfortunately, cost precludes the use of full ship shock trials on a routine basis and the few events of this type that can be staged are best used to validate predictive methods. The non-linearity and coupled nature of the problem do not make it amenable to purely empirical methods. For explosions that are far from the target, methods based on the DAA[1], such as the USA code[2], can be used. Such techniques estimate the explosive loads empirically and couple this analysis with a finite element target model that alters the loading based on the predicted deformation. However, for close-in explosions, the estimated DAA loading is not accurate and there is little recourse to a coupled Euler fluid/explosive model and a Lagrange structure simulation. At the end of each computational step, the Euler code passes the Lagrange code the loads on the surface structural nodes while the Lagrange code passes the node locations and velocities back.

Development of an underwater damage predictive capability requires developing as well as validating coupled hydrocodes. Validating data has been generated by a series of experiments that place an explosive inside a water filled cylinder[3]. These tests acquired transient pressure data in the water, transient deformation data on the cylinder mid-line and final deformation measurements along the cylinder. Although this experimental arrangement is simpler and smaller in scale than a ship or submarine, it exhibits target-shock loading and subsequent cavitation unloading that typifies underwater explosion-target interaction. Furthermore, its small size allows it to be conducted in a laboratory under ideal conditions, facilitating accurate data measurement.

It is reasonable to assume that accurately simulating these small-scale tests is a prerequisite to successfully predicting explosion damage to vessels.

The objective of the paper is to apply the GEMINI and DYSMAS hydrocode codes to the above water filled cylinder experiments and to compare calculation and measurement. The DYSMAS code has been developed by the IABG Corporation and is currently being maintained and enhanced in collaboration with the Warhead Performance and Lethality Division, Indian Head. The GEMINI code is a new code developed at Indian Head and based on the numerical method described in Ref. 4. Results shown in this paper described the predicted flow field evolution within the cylinder and the agreement between computed and measured cylinder deflection. An important feature of this comparison is determining the sensitivity of parameters that are not well known. These include the equation of state for water, cylinder material description as well as the JWL parameters and the initial explosive energy.

2. Description of Experiment

The experiment simulated in this paper is shown in Fig. 1, and described in detail in Ref. 3. It consists of a cylindrical tube containing water with a PETN explosive at its center. The cylinder is surrounded by air and its ends are covered by thin plastic sheets, initially containing the water. Instrumentation of relevance to this paper consists of a streak camera, a Laser interferometer and pressure gage. The streak camera views the edge of a cylinder through a slit and measures the mid-line deformation history while the laser interferometer measures radial velocity by detecting the Doppler induced frequency shift of light reflected from the cylinder surface. The pressure gage is affixed to the inner wall of the cylinder at the mid-line and provides pressure history at this point.

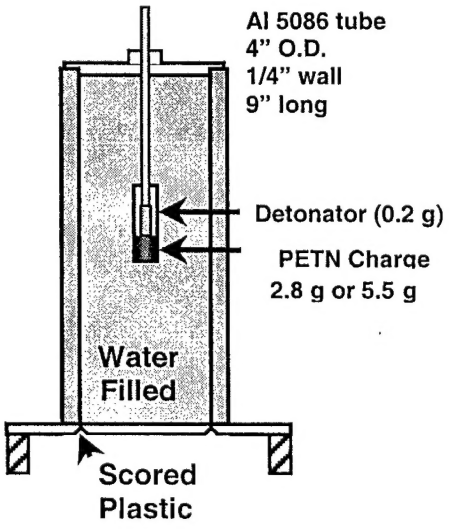

Figure 1. Water filled cylinder experiment.

Numerous experiments have been conducted with this and similar setups. This paper will compare to results with PETN explosive weights of 2.8 g and 5.5 g. To account for the .2 g weight of the detonator, these charges have been increased in the simulations to 3.0 g and 5.7 g, respectively. The streak camera and interferometer results are in close agreement with one another and only the camera results are used here.

3. Methodology

The GEMINI code is a time split, higher order Godunov method that employs both a Lagrange and re-map step. An outline of it is given in Ref .4. Coupled runs made with this code are executed as two separate processes; the GEMINI fluid code and the structure code. Information is exchanged between these processes at the end of every fluid computational step, allowing the structure code to sub-cycle if necessary. The interface coupling these two processes is termed the Standard Coupler Interface. It requires that nodal forces be passed from GEMINI to the structure code and node velocities and locations returned. Currently DYNA 2D, DYNA 3D and EPIC can accommodate the coupler interface.

The numerical method applied in the DYSMAS/E Euler code is based on work by Gentry, *et. al.*[5] It has been modified using flux corrected transport (FCT) and is coupled to DYSMAS/L, a Lagrange structure code that is similar to DYNA. Coupled runs with the DYSMAS code are compiled as a single executable with altered DYSMAS/E and DYSMAS/L main routines and a coupler module, DYSMAS/C, that presides over the calculation, handling data exchange between these two modules.

The Modified Tait[6] and Tillotson[7] equations of state are used to model water. These are as follows in cgs units:

Modified Tait: $p = p_0 + \omega\rho(e - e_0) - (\gamma B - \omega p_0)(1 - \rho / \rho_0)$

where $p_0 = 1(10^6)$, $\rho_0 = 1$, $\omega = 6.15$, $\gamma = 7.15$, $e_0 = 3.542(10^9)$, $B = 3.0479(10^9)$

Tillotson: $p = p_0 + \omega\rho(e - e_0) + A\mu + B\mu^2 + C\mu^3$

where $p_0 = 1(10^6)$, $\omega = .28$, $e_0 = 3.542(10^9)$, $A = 2.2(10^{10})$, $B = 9.94(10^{10})$, $C = 1.457(10^{11})$

The Modified Tait has been traditionally used in this project to describe water while the Tillotson equation has been recently devised to better fit high-pressure water data. These models use a simple pressure floor cavitation simulation. The pressure is prevented from being less than a

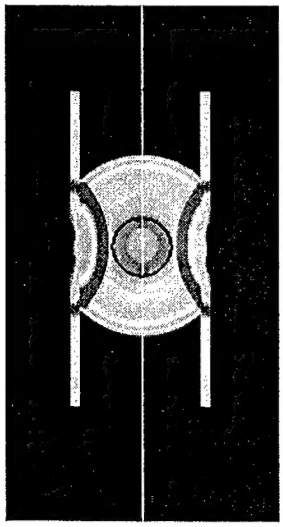

Figure 2. Pressure contours at 25 μsec.

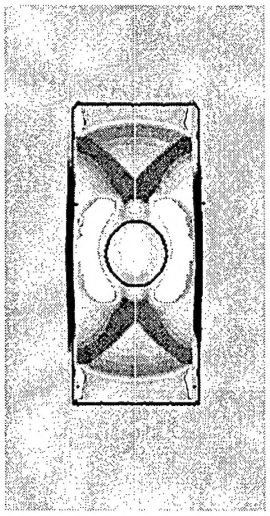

Figure 3. Pressure contours at 48 μsec.

prescribed cavitation level, however, the sound speed is calculated in the normal fashion.

Three different material models have been tested. The simplest is the Power Law Isotropic Elastic-Plastic model found in the DYNA 2D code[8]. This material behavior is elastic-plastic with non-linear isotropic strain hardening given by a power law expression. This model is not rate dependent. The second is the Mechanical Threshold Stress model[9] (MTS) that represents the flow stress of a material as the sum of different types of dislocation interactions: athermal stress associated with long-range barriers, mechanical threshold and thermal activation deformation. The third material model is a table lookup method. In the current work, MTS style curves were incorporated into the tables, however, the table entries were not based on that same material parameters used in the second model. Rather they were derived from tests made on a specimen of the material from which the cylinder was machined. The second and third models are designed MTS-1 and MTS-2, respectively.

Calculations made with the GEMINI code assume an instantaneous detonation while the DYSMAS code used both this approach and prescribed burn initiation, with the point of ignition located at the top edge of the charge.

4. Computational Description of Experiment

A computational description of the flow field evolution is given in Figs. 2 through 6. These results were generated by the GEMINI code coupled with the Epic MTS-1 model. Figs. 2, 3 and 4 show pressure contour plots at different times while Figs. 5 and 6 provide a record of the computed velocity and displacement of the cylinder mid-line.

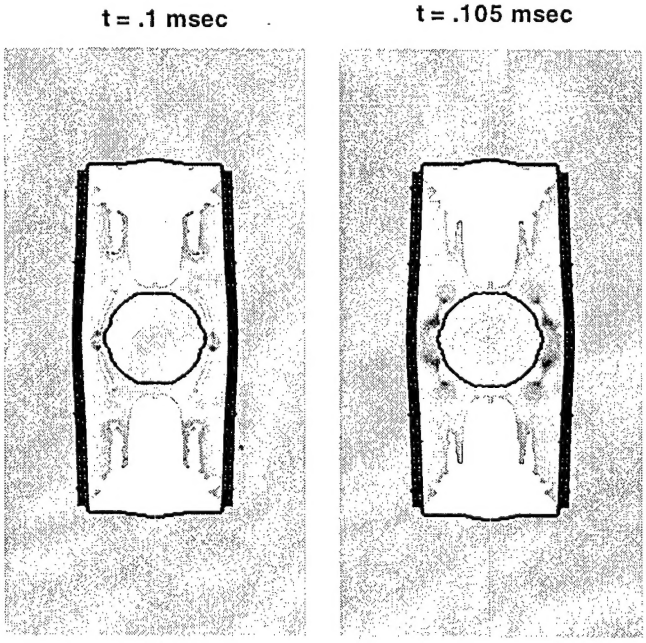

Figure 4. Pressure contour at cavitation collapse. White areas are cavitated regions.

The simulation commences with a detonation of the charge at the center of the cylinder. This explosion generates a shock that impacts the wall of the cylinder, accelerating it outwards. In the case of a rigid cylinder, this shock reflects off of the cylinder inner wall, producing a period of sustained, high pressure loading. In the present non-rigid case, the outward motion of the wall decreases the density of the surrounding water. Water is not very compressible and the extra volume created by the wall motion reduces the water pressure and unloads the wall. The resulting low-pressure region is illustrated in Fig. 2, while Fig. 5 demonstrates the accompanying decrease in acceleration (i.e. see "wall velocity induced unloading" label). The reflected shock interacts with the bubble and is itself reflected as an expansion the lowers the surrounding water pressure and produces a cavitation region, denoted by the white areas in Fig. 3. This intense region of low pressure reverses the direction of the acceleration as shown in Fig. 5. The wall deceleration ends with the advent of cavitation collapse. This phenomenon generates a new shock that impacts the cylinder and provides a short period of reloading. The cavitation collapse is illustrated in Fig. 4, while the increase in cylinder wall velocity accompanying the reloading is depicted in Fig. 5.

The sequence of events leading up to the first cavitation collapse is repeated several times as the flow field evolves within the cylinder. These cycles consist of the following events:

1. Shock forms and loads cylinder.
2. Shock reflects off of the wall and interacts with the bubble.
3. Shock reflects off the bubble as an expansion that form a cavitation region.
4. Cavitation region collapses forming of a new shock.

Subsequent instances of cavitation reloading are marked in Fig. 5 and 6. The primary difference between the first and later sequences is the mechanism forming the shock. In the first cycle, the shock is generated by the explosion, rather than by cavitation collapse.

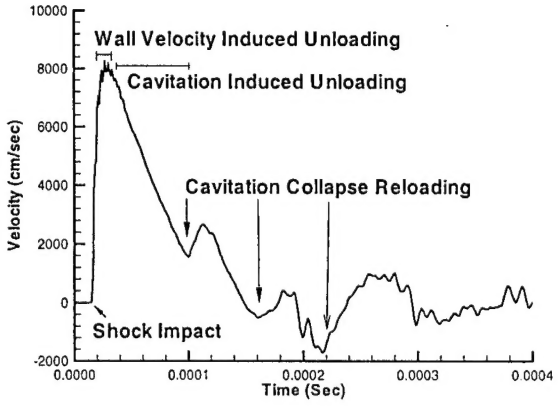

Figure 5. Computed mid-line wall velocity for the 2.8g test.

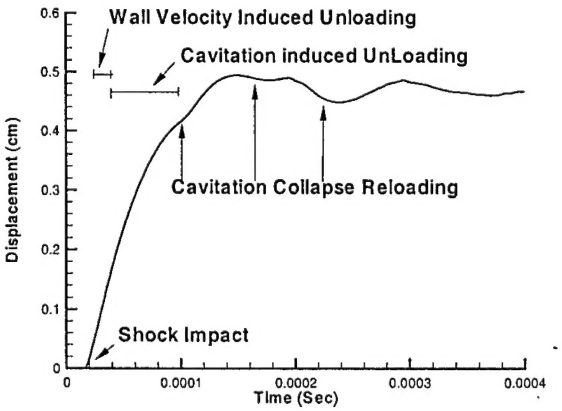

Figure 6. Computed mid-line wall displacement for the 2.8g test.

Quantitative Results

Results obtained with the GEMINI code coupled to DYNA 2D are shown in Figs. 7 through 10 for the 2.8g test. Here the Tillotson equation of state was used to model the water and the aluminum cylinder was simulated using the DYNA 2D Power Law Isotropic Elastic-Plastic model. Calculations were completed on a standard 100x200 Euler grid with 73 quadrilateral

DYNA elements and on a fine mesh with 200x400 Euler grid and 288 DYNA elements. As can be seen in Figs. 7 through 10, results on the two Euler grids are in close agreement with one another, indicating mesh converged results.

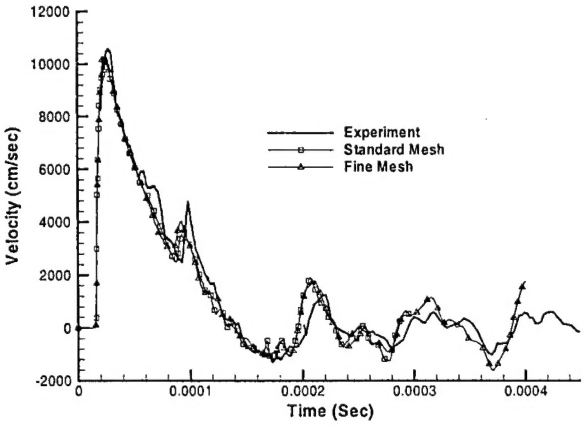

Figure 7. Computed mid-line wall velocity for the 2.8g test.

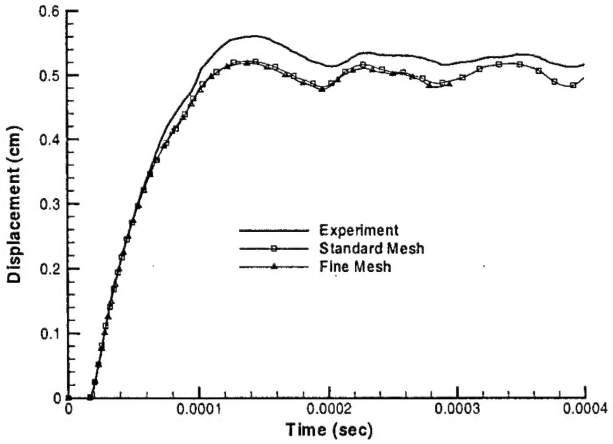

Figure 8. Computed mid-line wall deflection for the 2.8g test.

Figs. 7 and 8 illustrate the agreement between computed and measured mid-line velocity and displacement, respectively. Overall, the agreement is close, but the final measured deflection is greater than the computed one. Predicted and measured velocity and deflections agree well until about 50μsec, which is slightly prior to the first cavitation collapse. Here the measured mid-line wall velocity experiences an increment that is not seen in the calculation. Also, Fig. 7 demonstrates that the measured cavitation collapse and reloading is more forceful than in the predicted one.

Agreement between the measured and computed pressure at the wall is shown in Fig. 9. Here the calculated pressure is taken from the Euler code and is the pressure history at a point adjacent to the wall at the start of the calculation. The peak pressure values and overall pressure functional form agree well with experiment. Note that between .05 msec and .08 msec the experimental pressure exhibits an irregular positive value that corresponds to the irregular velocity at the same time in Fig. 7. Cavitation reloading accounts for the pressure rise between .08 and 1 msec.

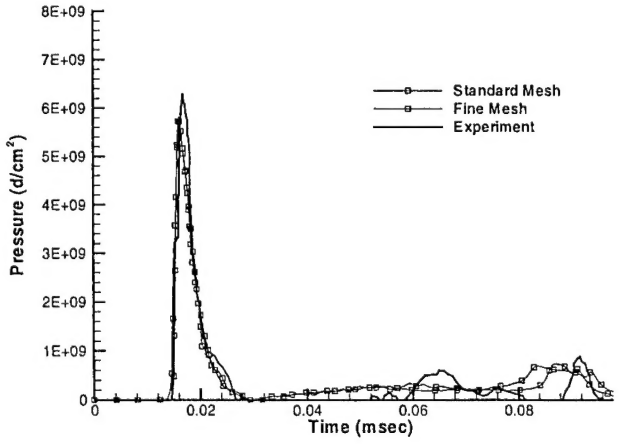

Figure 9. Mid-line wall pressure.

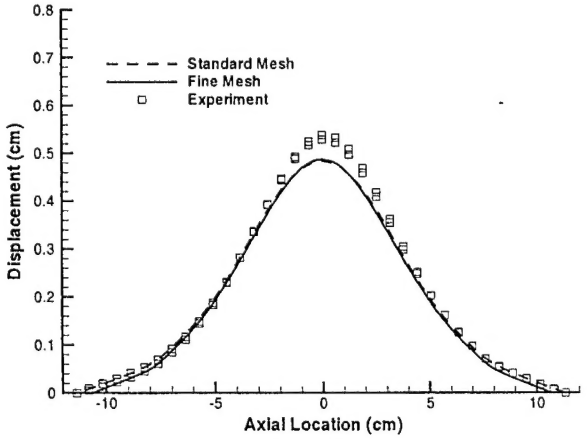

Figure 10. Final deflection versus length.

The final cylinder deformation as a function of cylinder length is shown in Fig. 10. Measurement and calculation are in reasonable agreement, except near the mid-line where the larger deflection shown in Fig. 8 is also visible here.

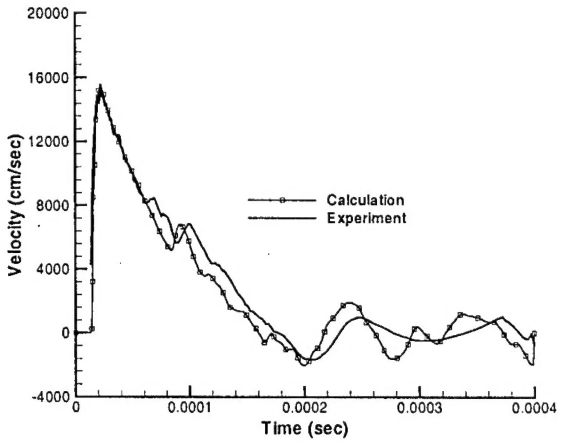

Figure 11. Mid-line velocity for the 5.5g test.

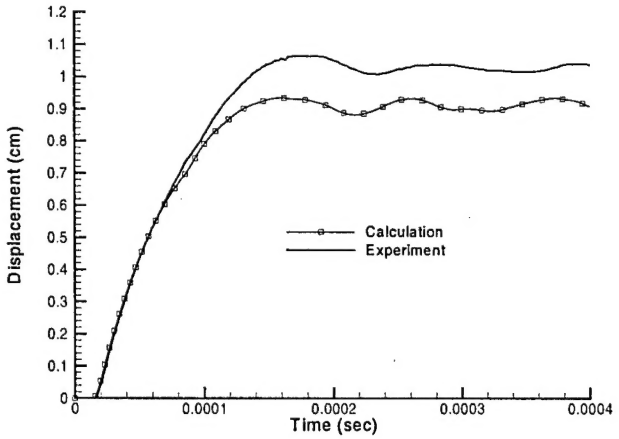

Figure 12. Mid-line displacement for the 5.5g test.

Cylinder mid-line velocity and displacement for the 5.5g test are shown in Figs. 11 and 12. Discrepancies between calculation and experiment are generically the same as in the 2.8g test. The computed and measured velocity are in good agreement prior to the first cavitation reloading, up to .06 msec. Here the measured velocity exhibits an increased, irregular value followed by cavitation reloading.

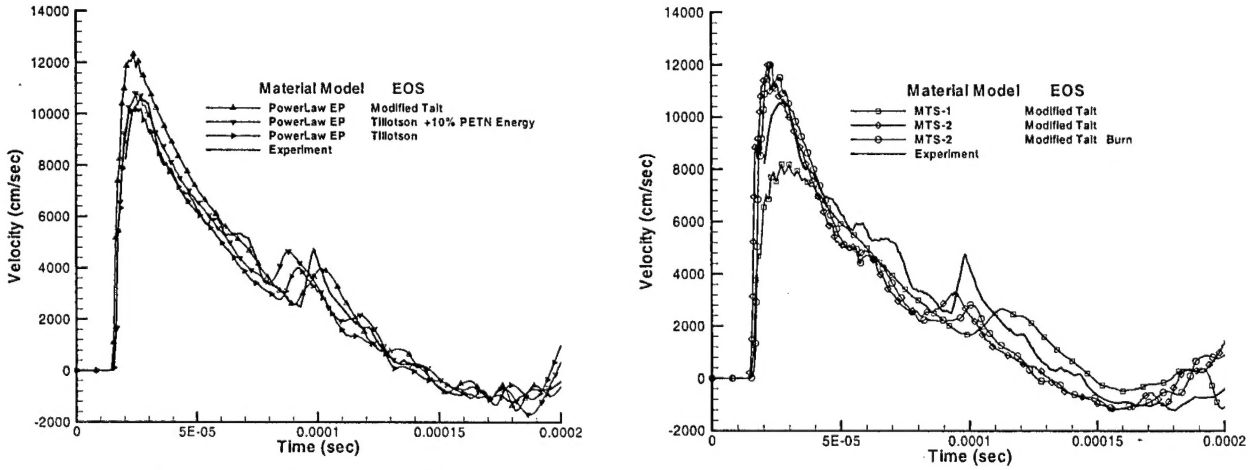

Figure 13. Sensitivity of mid-line velocity to model changes.

A degree of uncertainty surrounds some of modeling details used to obtain the quantitative results in Figs. 7 through 12. To assess the importance of such details, additional calculations have been made with the following changes:

1. water equation of state: Tillotson is replaced with the Modified Tait
2. material model: Power Law Isotropic Elastic-Plastic is replaced with MTS-1 and MTS-2
3. explosive energy: 10% increase in the explosive energy
4. burn model: inclusion of a prescribed burn model

Computed mid-line velocity and displacement are shown in Figs. 13 and 14. The cases labeled MTS-2 were completed with the DYSMAS code, while the remainder are GEMINI results.

An examination of Figs. 13 and 14 suggests that uncertainties concerning the water equation of state, material model and explosive energy can influence results significantly, changing the final deformation by up to 20%. Inclusion of a burn model effects the details of the velocity history a small amount, but has little impact on the mid-line displacement history.

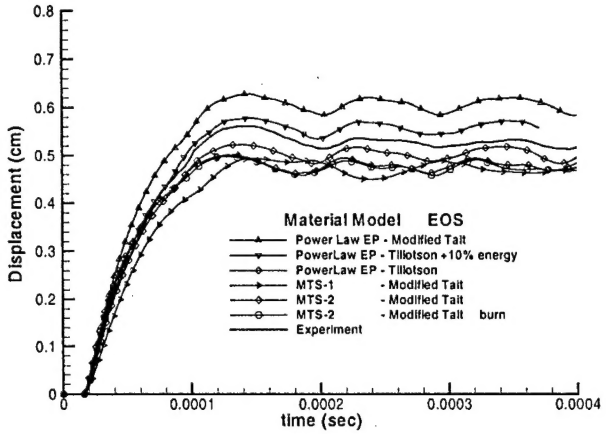

Figure 14. Sensitivity of mid-line displacement to model changes

5. Summary and Conclusions

Simulations have been conducted of an explosion within a water filled cylinder. This simulation indicates that the flow within the cylinder is dominated by an interaction between shock waves, the explosion bubble surface and cavitation regions. A shock wave interacts with the bubble to form an expansion that reduces pressures sufficiently to produce a cavitation region. This region subsequently collapses to form a new shock that reloads the structure. This cycle of events occurs several times, with the first cycle being initiated by the explosion shock and subsequent ones by shocks generated by cavitation collapse.

Good agreement is obtained between computation and experiment with regard to cylinder displacement, cylinder velocity, surface pressure and final cylinder shape. Also, repeating the computation with two different mesh sizes indicates that the solution on a moderate mesh is converged with respect to these observables. By repeating calculations with different water equations of state, material models and explosive energies, it is shown that uncertainties in defining these aspects of the model can have significant effects on results, changing the maximum deformation by up to 20%.

Acknowledgements

The authors would like to thank M. Borrman and R. Tewes of IABG for help in coupling GEMINI to DYNA 2-D and DYNA 3-D.

References

1. Geers,T.L., "Doubly Asymptotic Approximations of Transient Motions of Submerged Structures", **J. Accoust. Soc. Amer.**, 63, pp. 1500-1508, 1978.
2. DeRuntz, J. A., Geers, L. T., Felippa, C. A., "The Underwater shock Analysis Code (USA-Version 3)", DNA 5615F, Defense Nuclear Agency, Washington D.C.
3. Chambers, G.,Sandusky H., Zerrilli, F., Rye K., Tussing R.,"Pressure Measurements on a Deforming Surface in Response to an Underwater Explosion", CP429, **Shock Compression of Condensed Matter**, Ed. Schmidt, Dandekar, Forbes, the American Institute of Physics, 1998.
4. Wardlaw, A., "The 1-D Godunov Hydrocode Suite", IHTR 2088, Sep. 1998.
5. Gentry, A., Martin, R., and Daly, B., "An Eulerian Differencing Method for Unsteady Compressible Flow Problems", JCP, 1, 1966, pp. 87-118.
6. Fiessler, B., Dysmas Theory Manual
7. Fiessler, B., Private Communication, IABG, Nov. 9 1998.
8. Whirley, R., Engelman B., and Hallquist J. O., "DYNA-2D; A Nonlinear, Explicit Two-Dimensional Finite Element Code for Solid Mechanics, User Manual" Lawrence Livermore National Laboratory Report UCRL-MA 110630, April 1992.
9. Whirley, R., Engelman B., and Hallquist J. O., "DYNA-3D; A Nonlinear, Explicit Three-Dimensional Finite Element Code for Solid Mechanics, User Manual" Lawrence Livermore National Laboratory Report UCRL-MA 107254, November 1993.

PLEASE CHECK THE APPROPRIATE BLOCK BELOW:

-AQ #_____

☐ 1 copies are being forwarded. Indicate whether Statement A, B, C, D, E, F, or X applies.

☒ DISTRIBUTION STATEMENT A:
APPROVED FOR PUBLIC RELEASE: DISTRIBUTION IS UNLIMITED

☐ DISTRIBUTION STATEMENT B:
DISTRIBUTION AUTHORIZED TO U.S. GOVERNMENT AGENCIES ONLY; (Indicate Reason and Date). OTHER REQUESTS FOR THIS DOCUMENT SHALL BE REFERRED TO (Indicate Controlling DoD Office).

☐ DISTRIBUTION STATEMENT C:
DISTRIBUTION AUTHORIZED TO U.S. GOVERNMENT AGENCIES AND THEIR CONTRACTORS; (Indicate Reason and Date). OTHER REQUESTS FOR THIS DOCUMENT SHALL BE REFERRED TO (Indicate Controlling DoD Office).

☐ DISTRIBUTION STATEMENT D:
DISTRIBUTION AUTHORIZED TO DoD AND U.S. DoD CONTRACTORS ONLY; (Indicate Reason and Date). OTHER REQUESTS SHALL BE REFERRED TO (Indicate Controlling DoD Office).

☐ DISTRIBUTION STATEMENT E:
DISTRIBUTION AUTHORIZED TO DoD COMPONENTS ONLY; (Indicate Reason and Date). OTHER REQUESTS SHALL BE REFERRED TO (Indicate Controlling DoD Office).

☐ DISTRIBUTION STATEMENT F:
FURTHER DISSEMINATION ONLY AS DIRECTED BY (Indicate Controlling DoD Office and Date) or HIGHER DoD AUTHORITY.

☐ DISTRIBUTION STATEMENT X:
DISTRIBUTION AUTHORIZED TO U.S. GOVERNMENT AGENCIES AND PRIVATE INDIVIDUALS OR ENTERPRISES ELIGIBLE TO OBTAIN EXPORT-CONTROLLED TECHNICAL DATA IN ACCORDANCE WITH DoD DIRECTIVE 5230.25, WITHHOLDING OF UNCLASSIFIED TECHNICAL DATA FROM PUBLIC DISCLOSURE, 6 Nov 1984 (Indicate date of determination). CONTROLLING DoD OFFICE IS (Indicate Controlling DoD Office).

☐ This document was previously forwarded to DTIC on _____ (date) and the AD number is _____.

☐ In accordance with provisions of DoD instructions, the document requested is not supplied because:

☐ It will be published at a later date. (Enter approximate date, if known).

☐ Other. (Give Reason)

DoD Directive 5230.24, "Distribution Statements on Technical Documents," 18 Mar 87, contains seven distribution statements, as described briefly above. Technical Documents must be assigned distribution statements.

DR. JUDAH GOLDWASSER, ONR 333
Print or Type Name

SEE ATTACHED / 4-22-99
Authorized Signature/Date

(703) 696-2164
Telephone Number